Outage Analysis for Correlated Sources Coding over NOMA in Shadowed κ-μ Fading

Shen Qian, Jiguang He, Xiaobo Zhou, Takamasa Imai, Tad Matsumoto

Outage Analysis for Correlated Sources Coding over NOMA in Shadowed κ-μ Fading

Shen Qian*, Jiguang He† ‡, Xiaobo Zhou§, Takamasa Imai* and Tad Matsumoto¶
Email: shenqian@kanagawa-u.ac.jp
*Department of Information Systems Creation, Faculty of Engineering, Kanagawa University, Japan
†International Institute of Next Generation Internet, Macau University of Science and Technology, China
‡Centre for Wireless Communications, University of Oulu, Finland
§School of Computer Science and Technology, Tianjin University, China
¶IMT-Atlantic, Brest, France

***Abstract*—We consider correlated sources coding over a up-link non-orthogonal multiple access shadowed κ-μ fading channel. The sufficient condition for lossless coding is determined by the intersection of the Slepian-Wolf region and multiple access channel region, assuming source-channel separation holds. The exact expression for the outage probability upper bound is derived by dividing the sufficient conditions into three cases. The accuracy of the analytical results is verified by the Monte-Carlo simulations. The analytical results indicate that more than 2^{nd} order diversity gain can be achieved with a larger ratio of line-of-sight dominant component in single cluster or multiple clusters with non-line-of-sight component. It is also found that the shadowed κ-μ fading well represents one-sided Gaussian, Rayleigh, Rician, and Nakagami-m fading in calculating the outage probability. Furthermore, the ϵ-outage achievable rate is analyzed, which is found to be larger with higher source correlation and/or average signal-to-noise ratio.**

***Index Terms*—Up-link NOMA, shadowed κ-μ fading, Slepian-Wolf theorem, outage probability, ϵ-outage achievable rate**

I. Introduction

Non-orthogonal multiple access (NOMA) has been considered as a promising multiple access technique for the fifth generation (5G) and beyond 5G mobile networks. The basic concept of NOMA is that multiple users are served with the same wireless resource, such as a time slot, frequency, or an subcarrier [1]. Compared with the conventional orthogonal multiple access schemes which serves each user with orthogonal resource, NOMA can achieve higher spectral efficiency, larger system throughput, and lower transmission latency [2]. The connection capacity of Internet of Things (IoT) systems can be increased by NOMA compared to its orthogonal counterpart [3].

Most literature on NOMA assume the information sources to be transmitted are independent. However, in the emerging IoT applications, such as surveillance networks, smart agriculture or vehicle-to-everything (V2X) communications, the data sequences, obtained by the sensor nodes, are usually correlated with each other. For example, in smart agriculture scenario, the densely deployed sensors usually obtain the similar information since the sensor nodes are close to each other geographically. Recently, work about correlated source transmission with NOMA has attracted considerable attentions. The uplink NOMA with correlated sources can be regarded as many-to-one or reach back channel problem [4] since the correlated observations are available at the transmit nodes. The achievable rate region was analyzed in a cellular downlink NOMA transmission system with correlated information sources [5].

In particular, the coding schemes were proposed based on Slepian-Wolf or Wyner-Ziv coding, depending on whether a lossy or lossless recovery of these information sources is needed at the destination [6]. Ref. [7] employed a cooperative uplink NOMA to take advantage of the source/channel correlations by using an iterative joint detecting and decoding strategy at the receiver. The correlation among sources can be considered as a metric for user pairing and the spectral- and power-efficiency can be improved. A minimum mean square error (MMSE) detector was proposed in [8] for iterative joint detecting and decoding the correlated sources transmitted over asynchronous NOMA channels. Cheng *et al.* derived the outage probability of a lossy transmission of binary symmetric source with downlink NOMA and successive refinement [9]. Zhou *et al.* [10] and He *et al.* [11] calculated the outage probability upper bound for a two-correlated-source-coding system and for the two hop non-orthogonal multiple access relay channel, respectively, based on the derived sufficient condition. Furthermore, Song *et al.* [12] discussed the case where only one of the sources needs to be recovered at the destination, whereas the other source serves as a helper.

The previous work only assumed that the channels experienced non-line-of-sight fading and ignored the shadowing. However, in the IoT applications, wireless devices may be blocked by obstacles such as buildings or vegetation. Therefore, line-of-sight (LOS) and non-LOS components co-exist, in general, and the links will be heavily susceptible to possible deep fading caused by shadowing [13]. To the best of the authors' knowledge, the outage analysis of correlated source transmission in shadowed fading with the coexistence of both LOS and non-LOS components has not yet been reported in the literature.

In this work, we derived the outage probability upper bound of correlated source coding in uplink NOMA with shadowed κ-μ fading. The shadowed κ-μ fading [14] is an universal distribution model which contains other well-know fading

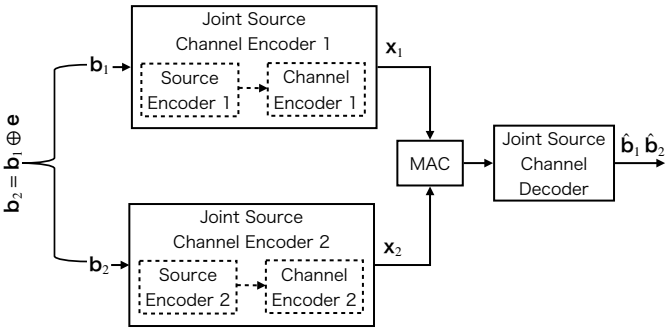

Fig. 1. An illustration of encoder and joint decoder for correlated sources coding over a MAC.

models such as the Rayleigh, Rician, Nakagami-m, and one-sided Guassion by specifying the three physical parameters, m, κ, and μ. The sufficient condition for lossless coding is determined by the intersection of the Slepian-Wolf region, and the multiple access channel (MAC) region by assuming that the source-channel separation holds. The analytical results indicate that more than 2^{nd} order diversity gain can be achieved with larger ratio of LOS dominant component in single cluster or multiple clusters with non-LOS component. The parameter specifications for shadowed κ-μ representing the one-side Gaussian, Rayleigh, Rician, κ-μ, and Nakagami-m fading models are verified by the outage performance. A comprehensive physical interpretation for the parameter specifications is provided. The analytical results are verified by Monte Carlo simulations.

II. System Model

A. Correlated Sources Coding with NOMA

We consider two correlated sources communicates with a common destination. Let $\mathbf{b}_1$ and $\mathbf{b}_2$ denote the original binary independently and identically distributed (i.i.d.) information sequences of the two sources, respectively. $\mathbf{b}_1$ and $\mathbf{b}_2$ are first encoded by their own source encoders, respectively, to representation patterns, which are then encoded to signal sequences $\mathbf{x}_1$ and $\mathbf{x}_2$ for transmitting to the destination over a multiple access channel. Thus, the information sequences $\mathbf{b}_1$ and $\mathbf{b}_2$ are received at the destination at the same time. The destination performs the joint decoding by utilizing the correlation between $\mathbf{b}_1$ and $\mathbf{b}_2$ once it receives the signal from the two nodes, as shown in Fig. 1 . Each node is assumed to be equipped with a single antenna.

The correlation between $\mathbf{b}_1$ and $\mathbf{b}_2$ is described, assuming $\mathbf{b}_2$ takes value from the output of a binary symmetric channel (BSC), with $\mathbf{b}_1$ being the channel input. The complementary parameter of the BSC channel is denoted by p ($p \in [0, 0.5]$), which also represents the correlation between $\mathbf{b}_1$ and $\mathbf{b}_2$. More specifically, p indicates the bit flipping probability between $\mathbf{b}_1$ and $\mathbf{b}_2$, as $\mathbf{b}_2 = \mathbf{b}_1 \oplus \mathbf{e}$, where $\oplus$ denotes the modulo-2 addition and $\mathbf{e}$ is the realizations of a binary random variable E where $\Pr(E = 1) = p$. Note that there is no channel between the two sources. A fixed bit flipping probability p is set as a parameter in this work.

TABLE I
Typical Fading Models Related to the κ-μ Shadowed Fading

Fading Model	m	κ	μ
Rayleigh	–	0	1
Rician	∞	K	1
Nakagami-m	–	0	m_{N}
κ-μ	∞	κ	μ
One-sided Gaussian	∞	0	0.5

B. Channel Model

We assume that the sources-to-destination links suffer from independent and identically distributed (i.i.d) shadowed κ-μ fading which considers the dominant component of the LOS path affected by the shadowing and subject to random fluctuations.

The probability density function of instantaneous signal-to-noise ratio (SNR) γ of the shadowed κ-μ fading is given by [14]

$$f_{\kappa\mu}(\gamma) = \frac{\mu^{\mu} m^m (1+\kappa)^{\mu}}{\Gamma(\mu)\bar{\gamma}(\mu\kappa + m)^m} \left(\frac{\gamma}{\bar{\gamma}}\right)^{\mu-1} \exp\left(-\frac{\mu(1+\kappa)\gamma}{\bar{\gamma}}\right) {}_1\mathrm{F}_1\left(m, \mu; \frac{\mu^2\kappa(1+\kappa)\gamma}{(\mu\kappa+\mu)\bar{\gamma}}\right), \quad (1)$$

where ${}_1\mathrm{F}_1(\cdot)$ and $\Gamma(\cdot)$ are the confluent hypergeometric function and Gamma function, respectively. $\bar{\gamma}$ denotes the average SNR. Here, the parameter m ($m \geq 0$) in (1) and (2) denotes the shadowing severity in the dominant components, where $m = 0$ indicates complete shadowing and $m \to \infty$ corresponds to no shadowing in the resultant dominant component. κ ($\kappa \geq 0$) denotes the ratio between the power of the dominant component to the total power of the scattered components and μ is the number of multipath clusters.

The cumulative density function of the shadowed κ-μ fading is given by [14]

$$F_{\kappa\mu}(\gamma) = \frac{\mu^{\mu-1} m^m (1+\kappa)^{\mu})}{\Gamma(\mu)(\mu\kappa + m)^m} \left(\frac{1}{\bar{\gamma}}\right)^{\mu} \Phi_2\left(\mu - m, m; \mu + 1; -\frac{\mu(1+\kappa)\gamma}{\bar{\gamma}}, -\frac{\mu(1+\kappa)m\gamma}{\bar{\gamma}(\mu\kappa + m)}\right), \quad (2)$$

where $\Phi_2(\cdot)$ is the bivariate confluent hypergeometric function.

By specializing the parameters m, κ, and μ in (1) and (2), some typical fading models can be obtained from the shadowed κ-μ fading. We show the parameter specializations for the shadowed κ-μ representing the one-side Gaussian, Rayleigh, Nakagami-m (with shape factor m_{N}) , κ-μ, and Rician (with Rician parameter K) in Table I and will demonstrate the validity of the value in Table I for outage calculations in the following sections.

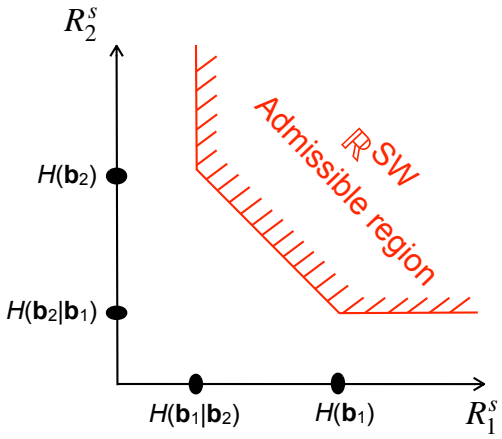

Fig. 2. Admissible region $\mathbb{R}^{\text{SW}}$ specified with Slepian-Wolf theorem.

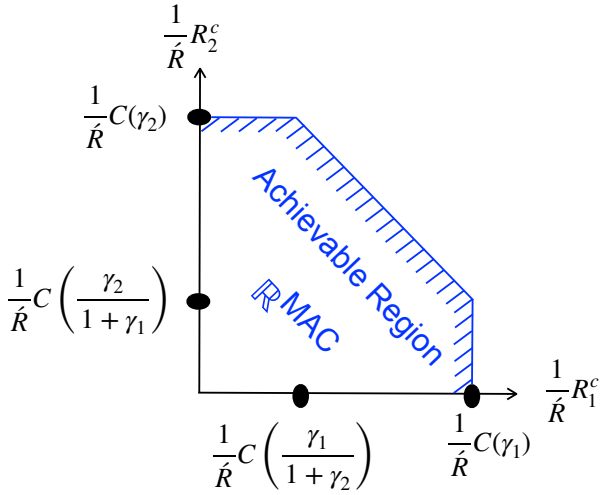

Fig. 3. Achievable region $\mathbb{R}^{\text{MAC}}$ of MAC transmission.

III. Outage Probability Analysis

In this section, we define the admissible rate region for the information of $\mathbf{b}_1$ and $\mathbf{b}_2$ and derive the outage probability upper bound of the Slepian-Wolf coding.

A. Admissible Rate Region for Source Coding

According to Shannon's source-channel separation theorem, the joint source-channel coding for $\mathbf{b}_1$ and $\mathbf{b}_2$ can be separated into a two-stage scheme: distributed source coding and MAC transmission. For the distributed lossless source coding, according to the Slepian-Wolf theorem, the admissible rate region is the set of source coding rate pair (R_1^s and R_1^s), satisfying the following inequalities:

$$\begin{cases} R_1^s & \geq H(\mathbf{b}_1|\mathbf{b}_2), \\ R_2^s & \geq H(\mathbf{b}_2|\mathbf{b}_1), \\ R_1^s + R_2^s & \geq H(\mathbf{b}_1, \mathbf{b}_2), \end{cases} \tag{3}$$

which is referred to as the Slepian-Wolf region $\mathbb{R}^{\text{SW}}$, as shown in Fig. 2. $H(\cdot|\cdot)$ and $H(\cdot,\cdot)$ denote the conditional and the joint entropy, respectively.

B. Achievable Capacity Region of MAC

The achievable capacity region of the MAC, $\mathbb{R}^{\text{MAC}}$, is defined as a closure of the convex hull of the rate pair (R_1^c and R_2^c) satisfying

$$\begin{cases} R_1^c & \leq C(\gamma_1), \\ R_2^c & \leq C(\gamma_2), \\ R_1^c + R_2^c & \leq C(\gamma_1 + \gamma_2), \end{cases} \tag{4}$$

where $C(\gamma) = \log_2(1+\gamma)$ is the channel capacity with the instantaneous SNR γ by assuming the dimension of the channel input is 1. R_i^c $(i \in (1,2))$ is the normalized spectrum efficiency including the channel coding rate and the modulation multiplicity of the corresponding channel. The region is illustrated as a bounded pentagonal, as shown in Fig. 3.

The sufficient condition for lossless coding of $\mathbf{b}_1$ and $\mathbf{b}_2$ is obtained by combining (3) with (4) as

$$\begin{cases} H(\mathbf{b}_1|\mathbf{b}_2)\acute{R} & \leq R_1^s\acute{R} \leq C(\gamma_1), \\ H(\mathbf{b}_2|\mathbf{b}_1)\acute{R} & \leq R_2^s\acute{R} \leq C(\gamma_2), \\ H(\mathbf{b}_1, \mathbf{b}_2)\acute{R} & \leq (R_1^s + R_2^s)\acute{R} \leq C(\gamma_1 + \gamma_2), \end{cases} \tag{5}$$

where $\acute{R}$ defines the total rate of the joint source-channel coding. For the sake of brevity, we assume that $\acute{R} = \acute{R}_1 = \acute{R}_2$, where $\acute{R}_1 = \frac{R_1^c}{R_1^s}$ and $\acute{R}_2 = \frac{R_2^c}{R_2^s}$. Eq. (5) indicates that if $\mathbb{R}^{\text{MAC}}$ and $\mathbb{R}^{\text{SW}}$ have an intersection as shown in Fig. 4, the success of the Slepian-Wolf coding over MAC can be guaranteed. On the contrary, the success of the Slepian-Wolf coding over a MAC can not be guaranteed when $\mathbb{R}^{\text{MAC}}$ and $\mathbb{R}^{\text{SW}}$ have no intersection with each other.

Since the source-channel separation theorem holds for point-to-point transmission in general, (5) is only the sufficient condition for transmitting one source with one helper over a MAC losslessly. This also leads to that the derived outage expression is the upper bound of practical performance.

C. Outage Probability Calculation

The destination can not guarantee the reconstruction of $\mathbf{b}_1$ with an arbitrarily small error probability when $\mathbb{R}^{\text{MAC}}$ and $\mathbb{R}^{\text{SW}}$ do not have an intersection, that is, $\mathbb{R}^{\text{MAC}} \cap \mathbb{R}^{\text{SW}} = \emptyset$. The outage event can be divided into three cases as shown in Fig. 5. The sufficient conditions of the three cases are expressed as

$$\begin{cases} \text{case 1}: \frac{C(\gamma_1)}{\acute{R}} < H(\mathbf{b}_1|\mathbf{b}_2), \\ \text{case 2}: H(\mathbf{b}_1|\mathbf{b}_2) < \frac{C(\gamma_1)}{\acute{R}} < H(\mathbf{b}_1), \frac{C(\gamma_1+\gamma_2)}{\acute{R}} < H(\mathbf{b}_1, \mathbf{b}_2), \\ \text{case 3}: H(\mathbf{b}_1) < \frac{C(\gamma_1)}{\acute{R}}, \frac{C(\gamma_2)}{\acute{R}} < H(\mathbf{b}_1|\mathbf{b}_2), \end{cases} \tag{6}$$

according to (5). In case 1, since $\frac{C(\gamma_1)}{\acute{R}}$ is smaller than $H(\mathbf{b}_1|\mathbf{b}_2)$, the outage always happens regardless of the value of $\frac{C(\gamma_2)}{\acute{R}}$. In case 2 and case 3, the outage events related to both the value of $\frac{C(\gamma_1)}{\acute{R}}$ and $\frac{C(\gamma_2)}{\acute{R}}$. Since $\frac{C(\gamma_1)}{\acute{R}} < H(\mathbf{b}_1|\mathbf{b}_2)$,

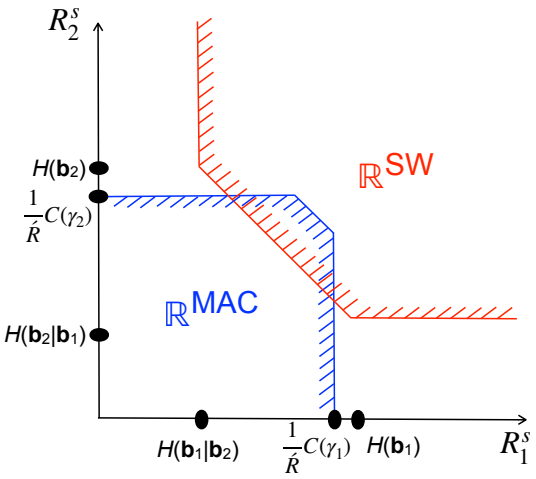

Fig. 4. No outage when $\mathbb{R}^{\text{MAC}} \cap \mathbb{R}^{\text{SW}} != \emptyset$.

$H(\mathbf{b}_1|\mathbf{b}_2) < \frac{C(\gamma_1)}{\acute{R}} < H(\mathbf{b}_1)$ and $H(\mathbf{b}_1) < \frac{C(\gamma_1)}{\acute{R}}$ are distinctive, the outage probability $\text{P}_{\text{out}}^{\text{shadowed }\kappa-\mu}$ of Slepian-Wolf coding in NOMA shadowed κ-μ fading is expressed as

$$\begin{aligned}\text{P}_{\text{out}}^{\text{shadowed }\kappa-\mu} &= \text{P}_{\text{case 1}}^{\text{out}} + \text{P}_{\text{case 2}}^{\text{out}} + \text{P}_{\text{case 3}}^{\text{out}} \\ &= \Pr\left\{\frac{C(\gamma_1)}{\acute{R}} < H(\mathbf{b}_1|\mathbf{b}_2)\right\} \\ &+ \Pr\left\{H(\mathbf{b}_1|\mathbf{b}_2) < \frac{C(\gamma_1)}{\acute{R}} < H(\mathbf{b}_1), \right. \\ &\left. \frac{C(\gamma_1+\gamma_2)}{\acute{R}} < 1 + H(\mathbf{b}_1|\mathbf{b}_2)\right\} \\ &+ \Pr\left\{H(\mathbf{b}_1) < \frac{C(\gamma_1)}{\acute{R}}, \frac{C(\gamma_2)}{\acute{R}} < H(\mathbf{b}_1|\mathbf{b}_2)\right\}. \end{aligned} \tag{7}$$

With the assumption that Gaussian code book is used, the relationship between the instantaneous channel SNR γ_i $(i \in (1,2))$ and its corresponding rates $\acute{R}$ are written as $\acute{R} \cdot H(\mathbf{b}_1) = \log_2(1+\gamma_1)$ and $\acute{R} \cdot H(\mathbf{b}_2) = \log_2(1+\gamma_2)$. Then, with the assumption that each link experiences statistically independent block fading, the outage probability is written as

$$\begin{aligned}\text{P}_{\text{case 1}}^{\text{out}} &= \int_0^{2^{\acute{R}H(p)}-1} f_{\kappa\mu}(\gamma_1)d\gamma_1 \\ &= \frac{\mu_1^{\mu_1-1} m_1^{m_1}(1+\kappa)^{\mu_1})}{\Gamma(\mu_1)(\mu_1\kappa_1+m_1)^{m_1}} \left(\frac{1}{\bar{\gamma}_1}\right)^{\mu_1} \\ &\cdot \Phi_2\left(\mu_1 - m_1, m_1; \mu_1+1; -\frac{\mu_1(1+\kappa_1)\left(2^{\acute{R}H(p)}-1\right)}{\bar{\gamma}_1}, \right. \\ &\left. -\frac{\mu_1(1+\kappa_1)m_1\left(2^{\acute{R}H(p)}-1\right)}{\bar{\gamma}_1(\mu_1\kappa+m_1)}\right), \end{aligned} \tag{8}$$

$$\begin{aligned}\text{P}_{\text{case 2}}^{\text{out}} &= \int_0^{2^{\acute{R}H(p)}-1} f_{\kappa\mu}(\gamma_1) \int_0^{2^{\acute{R}(1+H(p))}-1-\gamma_1} f_{\kappa\mu}(\gamma_2)d\gamma_2 d\gamma_1 \\ &= \int_0^{2^{\acute{R}H(p)}-1} \frac{\mu_1^{\mu_1} m_1^{m_1}(1+\kappa_1)^{\mu_1}}{\Gamma(\mu_1)\bar{\gamma}_1(\mu_1\kappa_1+m_1)^{m_1}} \left(\frac{\gamma_1}{\bar{\gamma}_1}\right)^{\mu_1-1} \\ &\cdot \exp\left(-\frac{\mu_1(1+\kappa_1)\gamma_1}{\bar{\gamma}_1}\right) {}_1\text{F}_1\left(m_1, \mu_1; \frac{\mu_1^2\kappa_1(1+\kappa_1)\gamma_1}{(\mu_1\kappa_1+\mu_1)\bar{\gamma}_1}\right) \\ &\cdot \frac{\mu_2^{\mu_2-1} m_2^{m_2}(1+\kappa_2)^{\mu_2})}{\Gamma(\mu_2)(\mu_2\kappa_2+m_2)^{m_2}} \left(\frac{1}{\bar{\gamma}_2}\right)^{\mu_2} \\ &\cdot \Phi_2\left(\mu_2 - m_2, m_2; \mu_2+1; -\frac{\mu_2(1+\kappa_2)\left(2^{\acute{R}(1+H(p))}-1-\gamma_1\right)}{\bar{\gamma}_2}, \right. \\ &\left. -\frac{\mu_2(1+\kappa_2)m_2\left(2^{\acute{R}(1+H(p))}-1-\gamma_1\right)}{\bar{\gamma}_2(\mu_2\kappa_2+m_2)}\right) d\gamma_1 \end{aligned} \tag{9}$$

and

$$\begin{aligned}\text{P}_{\text{case 3}}^{\text{out}} &= \int_{2^{\acute{R}}-1}^{\infty} f_{\kappa\mu}(\gamma_1)d\gamma_1 \int_0^{2^{\acute{R}H(p)}-1} f_{\kappa\mu}(\gamma_2)d\gamma_2 \\ &= \left[1 - \frac{\mu_1^{\mu_1-1} m_1^{m_1}(1+\kappa)^{\mu_1})}{\Gamma(\mu_1)(\mu_1\kappa_1+m_1)^{m_1}} \left(\frac{1}{\bar{\gamma}_1}\right)^{\mu_1} \right. \\ &\cdot \Phi_2\left(\mu_1 - m_1, m_1; \mu_1+1; -\frac{\mu_1(1+\kappa_1)\left(2^{\acute{R}}-1\right)}{\bar{\gamma}_1}, \right. \\ &\left.\left. -\frac{\mu_1(1+\kappa_1)m_1\left(2^{\acute{R}}-1\right)}{\bar{\gamma}_1(\mu_1\kappa+m_1)}\right)\right] \\ &\cdot \frac{\mu_2^{\mu_2-1} m_2^{m_2}(1+\kappa_2)^{\mu_2})}{\Gamma(\mu_2)(\mu_2\kappa_2+m_2)^{m_2}} \left(\frac{1}{\bar{\gamma}_2}\right)^{\mu_2} \\ &\cdot \Phi_2\left(\mu_2 - m_2, m_2; \mu_2+1; -\frac{\mu_2(1+\kappa_2)\left(2^{\acute{R}H(p)}-1\right)}{\bar{\gamma}_2}, \right. \\ &\left. -\frac{\mu_2(1+\kappa_2)m_2\left(2^{\acute{R}H(p)}-1\right)}{\bar{\gamma}_2(\mu_2\kappa_2+m_2)}\right). \end{aligned} \tag{10}$$

Since the derivation of the explicit expression of $\text{P}_{\text{case 2}}^{\text{out}}$ and $\text{P}_{\text{case 3}}^{\text{out}}$ is excessively complex, we use the recursive adaptive Simpson quadrature algorithm to numerically calculate the integrals in (9) and (10). Note that infinite frame length is assumed, which results in the derived outage probability are the upper bounds for the performance of the practical signaling schemes. Therefore, the analytical results in this work serve as references in practical coding/decoding design for transmitting correlated sources over fading MAC.

IV. Numerical Results and Discussions

Fig. 6 shows the outage performance in shadowed κ-μ fading comparing with those in one-sided Gaussian, Rician, and Nakagami-m fading. In the shadowed κ-μ fading, the parameters are set as $\kappa_1 = \kappa_2 = 0$, $\mu_1 = \mu_2 = 0.5$, and $m_1 = m_2 = \infty$ for comparing with one-sided Gaussian channel; the parameters are set as $\kappa_1 = \kappa_2 = 3$, $\mu_1 = \mu_2 = 1$, and $m_1 = m_2 = \infty$ for comparing with Rician channel; the parameters are set as $\kappa_1 = \kappa_2 = 0$, $\mu_1 = \mu_2 = 3$ for comparing with Nakagami-m channel. Correspondingly, the factor in Rician channel is set as $K = 3$ and the shape factor in Nakagami-m channel is set as $m_{\text{N}} = 5$. We observe that with the parameter specifications indicated in Table I, the

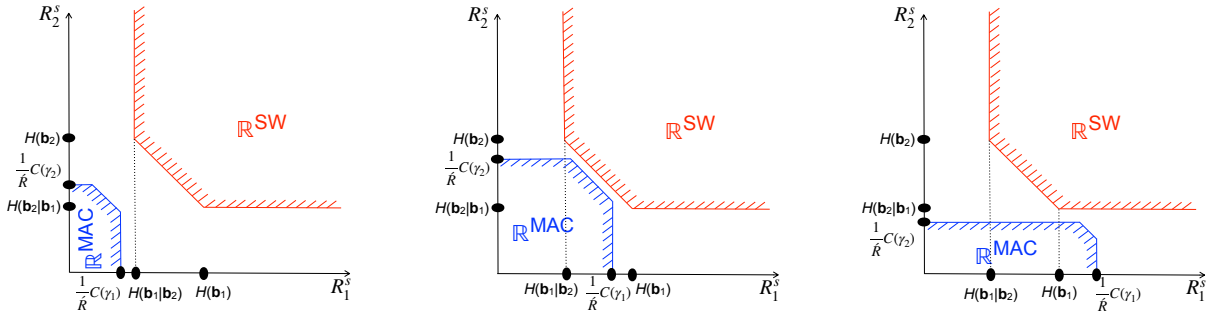

Fig. 5. Outage occurs when $\mathbb{R}^{\text{MAC}} \cap \mathbb{R}^{\text{SW}} = \emptyset$. (a) case 1: $H(\mathbf{b}_1|\mathbf{b}_2)\acute{R} \leq R_1^s\acute{R} \leq C(\gamma_1)$; (b) case 2: $H(\mathbf{b}_1|\mathbf{b}_2) < \frac{C(\gamma_1)}{\acute{R}} < H(\mathbf{b}_1)$, $\frac{C(\gamma_1+\gamma_2)}{\acute{R}} < 1 + H(\mathbf{b}_1|\mathbf{b}_2)$; (c) case 3: $H(\mathbf{b}_1) < \frac{C(\gamma_1)}{\acute{R}}, \frac{C(\gamma_2)}{\acute{R}} < H(\mathbf{b}_1|\mathbf{b}_2)$.

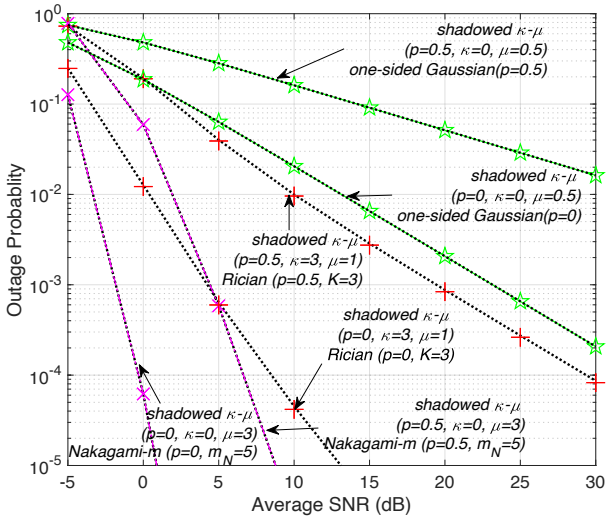

Fig. 6. Outage probability versus average SNR (dB) in different fading, where $\overline{\gamma}_1 = \overline{\gamma}_2$. $\kappa = \kappa_1 = \kappa_2 = 0$, $\mu = \mu_1 = \mu_2 = 0.5$, and $m = m_1 = m_2 = \infty$ for one-sided Gaussian; $\kappa = \kappa_1 = \kappa_2 = 3$, $\mu = \mu_1 = \mu_2 = 1$, and $m = m_1 = m_2 = \infty$ for Rician faidng with $K = 3$; $\kappa = \kappa_1 = \kappa_2 = 0$ $\mu = \mu_1 = \mu_2 = 3$ for Nakagami-m fading with shape factor $m_{\text{N}} = 5$.

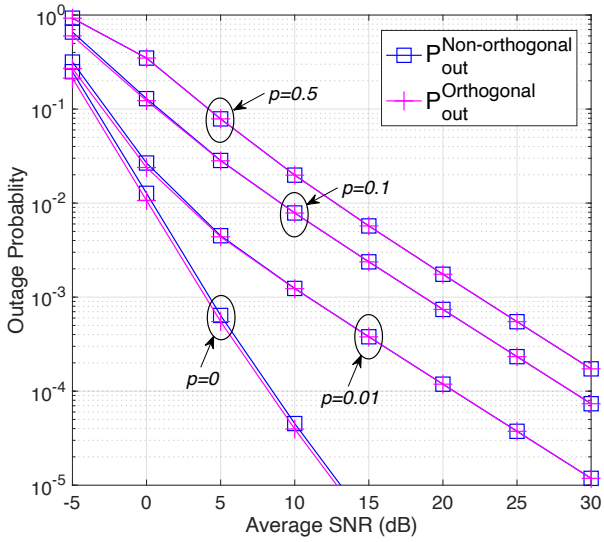

Fig. 7. Comparison between the outage probabilities of orthogonal and non-orthogonal transmission, where $\overline{\gamma}_1 = \overline{\gamma}_2$. $\kappa = \kappa_1 = \kappa_2 = 3$, $\mu = \mu_1 = \mu_2 = 1$, and $m = m_1 = m_2 = \infty$.

shadowed κ-μ well represents the one-sided Gaussian, Rician, and Nakagami-m, both in the fully correlated sources case ($p = 0$) and in the independent sources case ($p = 0.5$), with both non-LOS and LOS components existing in the channels. It is also found that the more than 2$^{\text{nd}}$ diversity order can be achieved with larger ratio of LOS dominant component in single cluster ($\kappa = 3, \mu = 1$) or with multiple clusters with non-LOS component ($\kappa = 0, \mu = 3$).

Fig. 7 plots the theoretical outage probability against the average SNR with the parameter p varying from 0 to 0.5. The outage probabilities of correlated source transmission over orthogonal channels are offered as benchmarks. From the outage curves, we could observe that the orthogonal transmission outperforms its non-orthogonal counterpart when the two sources are highly correlated (small p). It indicates that the correlation between the two sources is exploited at the destination. In contrast, when the correlation decreases (larger p), the advantage of orthogonal transmission over non-orthogonal transmission disappears in terms of the outage performance. However, with the same p, the same diversity gain can be observed in the outage curves with either orthogonal or non-orthogonal transmission.

Fig. 8 plots the outage probabilities with different parameters (κ, μ, and m) in shadowed κ-μ fading. It is shown that with $\kappa = \kappa_1 = \kappa_2 = 0$ and $\mu = \mu_1 = \mu_2 = 1$ as Rayleigh fading, $\kappa = \kappa_1 = \kappa_2 = 2$, $\mu = \mu_1 = \mu_2 = 1$, and $m_1 = m_2 = \infty$ as Rician faidng, and $\kappa_1 = \kappa_2 = 0$ and $\mu = \mu_1 = \mu_2 = 2$ as Nakagami-m fading, the Monte Carlo simulation results are in excellent agreement with the analytical results.

The ϵ-outage achievable rates with respect to the average SNR are shown in Fig. 9, where ϵ is set at 0.01. It is observed that for the same p, the ϵ-outage achievable rate increases as the average SNR increases. It is also found that the ϵ-

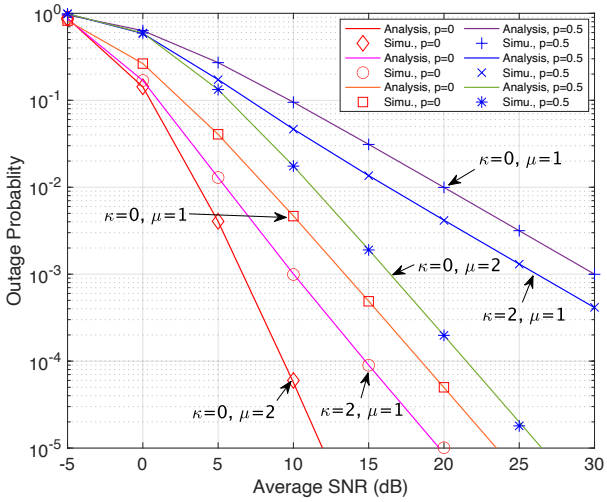

Fig. 8. Outage probability and versus average SNR (dB) with different parameters in shadowed κ-μ fading, where $\overline{\gamma}_1 = \overline{\gamma}_2$. $\kappa = \kappa_1 = \kappa_2 = 0$ and $\mu = \mu_1 = \mu_2 = 1$ for Rayleigh; $\kappa = \kappa_1 = \kappa_2 = 2$, $\mu = \mu_1 = \mu_2 = 1$, and $m_1 = m_2 = \infty$ for Rician; $\kappa = \kappa_1 = \kappa_2 = 0$ and $\mu = \mu_1 = \mu_2 = 2$ for Nakagami-m.

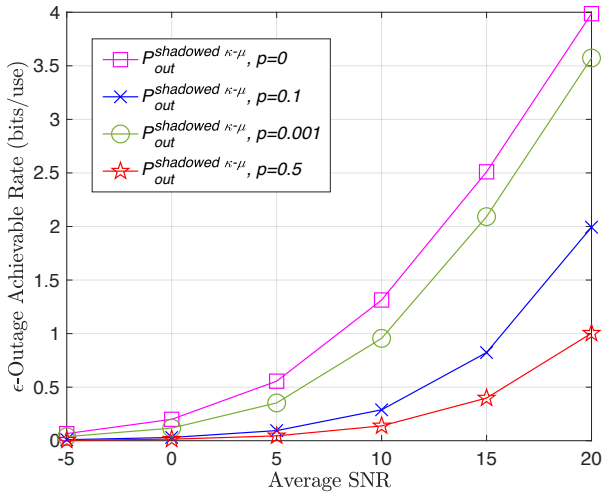

Fig. 9. ϵ-outage achievable rate versus average SNR (dB) as a function of p, where $\overline{\gamma}_1 = \overline{\gamma}_2$ and $\epsilon = 0.01$. $\kappa_1 = \kappa_2 = 1$, and $\mu_1 = \mu_2 = 1$, and $m_1 = m_2 = 1$.

outage achievable rate decreases as the values of p increase (the sources correlation becomes smaller). This indicates that with higher average SNR, the source correlation can be more utilized to eliminate redundancy after source coding, which leads to higher ϵ-outage achievable rate.

V. Conclusion

In this work, we have analyzed the outage probability for the Slepian-Wolf coding over up-link NOMA shadowed κ-μ fading channel. The outage probability upper bound expression has been derived based on the sufficient condition for lossless coding determined by the intersection of the Slepian-Wolf region and the multiple access channel region. It has been found that the outage performance of the orthogonal transmission is superior compared to its non-orthogonal counterpart with high correlation between the two sources. The ϵ-outage achievable rate increases with increasing the average SNR and/or with increasing the source correlation. The accuracy of the analytical results has been verified by a series of Monte Carlo simulations.

Only two correlated sources case is considered in this work, a promising future direction is to extend to the multiple correlated sources scenario by utilizing multiple-user MAC and multiple-source Slepian-Wolf theorem.

Acknowledgment

This research was supported in part by Japan Society for the Promotion of Science, KAKENHI 21K17738, and also in part by the National Natural Science Foundation of China under Grant 62072330.

References

[1] D. Wan, M. Wen, F. Ji, H. Yu, and F. Chen, "Non-orthogonal multiple access for cooperative communications: Challenges, opportunities, and trends," *IEEE Wireless Commun. Mag.*, vol. 25, no. 2, pp. 109–117, Jan. 2018.

[2] Y. Saito, A. Benjebbour, Y. Kishiyama, and T. Nakamura, "System-level performance evaluation of downlink non-orthogonal multiple access (NOMA)," in *Proc. IEEE Int. Symp. Pers., Indoor, Mobile Radio Commun.*, London, UK, Nov. 2013, pp. 611–615.

[3] A. E. Mostafa, Y. Zhou, and V. W. S. Wong, "Connectivity maximization for narrowband iot systems with NOMA," in *Proc. IEEE Int. Conf. Commun.*, Paris, France, July 2017, pp. 1–6.

[4] A. D. Murugan, P. K. Gopala, and H. E. Gamal, "Correlated sources over wireless channels: cooperative source-channel coding," *IEEE J. Select. Areas Commun.*, vol. 22, no. 6, pp. 988–998, Aug. 2004.

[5] K. Chung, "Noma for correlated information sources in 5g systems," *IEEE Commun. Lett.*, vol. 25, no. 2, pp. 422–426, Sept. 2021.

[6] M. H. Yassaee and M. R. Aref, "Slepian-wolf coding over cooperative relay networks," *IEEE Trans. Inform. Theory*, vol. 57, no. 6, pp. 3462–3482, Aug. 2011.

[7] N. Ahmad Khan Beigi and M. R. Soleymani, "Ultra-reliable energy-efficient cooperative scheme in asynchronous NOMA with correlated sources," *IEEE Internet of Things Journal*, vol. 6, no. 5, pp. 7849–7863, 2019.

[8] N. A. Khan Beigi and M. R. Soleymani, "NOMA-based network coding in IoT networks with correlated sources," in *Proc. IEEE Consumer Commun. Networking Conf.*, Las Vegas, USA, Jan. 2020, pp. 1–2.

[9] M. Cheng, W. Lin, and T. Matsumoto, "Down-link NOMA with successive refinement for binary symmetric source transmission," *IEEE Trans. Commun.*, vol. 68, no. 12, pp. 7927–7937, Sept. 2020.

[10] X. Zhou, X. He, M. Juntti, and T. Matsumoto, "Outage probability of correlated binary source transmission over fading multiple access channels," in *Proc. IEEE Works. on Sign. Proc. Adv. in Wirel. Comms.*, Stockholm, Sweden, June 2015, pp. 96–100.

[11] J. He, V. Tervo, S. Qian, Q. Xue, M. Juntti, and T. Matsumoto, "Performance analysis of lossy decode-and-forward for non-orthogonal MARCs," *IEEE Trans. Wireless Commun.*, vol. 17, no. 3, pp. 1545–1558, Dec. 2018.

[12] S. Song, M. Cheng, J. He, X. Zhou, and T. Matsumoto, "Outage probability of one-source-with-one-helper sensor systems in block rayleigh fading multiple access channels," *IEEE Sensors J.*, vol. 21, no. 2, pp. 2140–2148, Aug. 2021.

[13] J. Zeng, T. Lv, R. P. Liu, X. Su, Y. J. Guo, and N. C. Beaulieu, "Enabling ultrareliable and low-latency communications under shadow fading by massive MU-MIMO," *IEEE Internet of Things Journal*, vol. 7, no. 1, pp. 234–246, Oct. 2020.

[14] J. F. Paris, "Statistical characterization of $\kappa-\mu$ shadowed fading," *IEEE Trans. Veh. Technol.*, vol. 63, no. 2, pp. 518–526, Feb. 2014.